Int J Fract (2011) 171:185–193
DOI 10.1007/s10704-011-9638-2

ORIGINAL PAPER

# The theory of multiple peeling

**Nicola M. Pugno**

Received: 28 July 2011 / Accepted: 11 October 2011 / Published online: 15 November 2011


**Abstract** In this paper we derive the theory of multiple peeling, extending the pioneering energy-based single peeling theory of Kendall, including large deformations and pre-stretching. We can thus treat a complex system of films, adhering over a substrate and having a common hinge where the pulling force is applied. Two case studies are investigated: the asymmetric V-shape double peeling and the symmetric cone-shape configuration with $N$ peeling tapes, both requiring the solution of six nonlinear coupled equations (instead of the one needed in the simpler single peeling problem). Remarkable implications emerge: (1) for moderate deformations, the critical strain of a tape is identical to that of the single peeling; (2) an optimal peeling angle, at which adhesion is maximal, is discovered; (3) an additional optimization, even for hierarchical structures, is introduced by imposing the delamination force equal to the intrinsic fracture of the tape. Also, the length of the peeling process zone is calculated, suggesting different optimal values for flaw-tolerant peeling at different angles. Applications to gecko adhesion, for which the flaw-tolerant peeling is demonstrated, and spider silk anchors, that we are going to discuss in details in subsequent papers, are envisioned (including a new pre-stretching mechanism for adhesion control) and suggested by the evidence of a smart mechanism capable of maximizing adhesion simply by increasing the applied tension.

**Keywords** Multiple peeling · Adhesion · Geckos · Spider silk · Anchorages · Optimal · Smart

N. M. Pugno (✉)
Laboratory of Bio-inspired Nanomechanics "Giuseppe Maria Pugno", Department of Structural Engineering and Geotechnics, Politecnico di Torino, Corso Duca degli Abruzzi 24, 10129 Torino, Italy
e-mail: nicola.pugno@polito.it

N. M. Pugno
National Institute of Nuclear Physics, National Laboratories of Frascati, Via E. Fermi 40, 00044 Frascati, Italy

N. M. Pugno
National Institute of Metrological Research, Strada delle Cacce 91, 10135 Torino, Italy

## 1 Introduction

In spite of the general interest on peeling, especially in the fracture mechanics community, the seminal approach by Kendall (1975) remains the universally adopted theory for studying the single peeling. Its extension to multiple peeling has never been formulated and is the aim of the present paper. Such extension is of great importance per se but it is also motivated by the increasing interest in the study of the adhesion of biological and complex systems (see Israelachvili 1991) such as living animals: insects, spiders and geckos adhesion is in fact usually activated by controlateral legs, digits and even setae, which undoubtedly form a double more than a single peeling system.

In particular, hairy attachment systems of insects, arachnids and reptiles have been intensively studied during the past years (Autumn and Peattie 2002; Eisner and Aneshansley 2000; Federle et al. 2000; Glassmaker et al. 2004; Huber et al. 2005a; Kesel et al. 2004; Yao and Gao 2006; Chen and Gao 2007; Pugno 2007a; Pugno and Lepore 2008a,b; Bhushan and Sayer 2007), aiming to explain and possibly mimic their extraordinary adhesive abilities (Geim et al. 2003) even at the human size-scale thus towards the development of spiderman suit like tissues (Pugno 2007b, 2008). These systems consist of arrays of hierarchical hairs or setae, which allow for a large contact area on almost any even flat surface and hence feature high adhesion and friction, derived from a combination of van der Waals interaction (Autumn et al. 2002) and capillary attractive forces (Huber et al. 2005b). The smallest hierarchical level of seta is responsible for the formation of intimate contact with the substrate and appears as one or more tape-like two dimensional terminal elements of mostly spatulae shape (see Gorb 2001). Based on the studies of different animal groups, an interesting correlation between the geometrical properties of setal tips and animal weight was found thanks to the JKR model of contact mechanics (Johnson et al. 1971): the heavier the animal, the smaller and more densely packed the tips (Arzt et al. 2003). This scaling law was explained by introducing the principle of contact splitting, according to which splitting up the contact into finer sub-contacts increases adhesion. This concept has recently been adapted invoking the single peeling model of Kendall (1975), in order to explain why most biological hairy adhesive systems involved in locomotion rely on spatula-shaped terminal elements (Varenberg et al. 2010). In particular, we examined the contact formed between a smooth substrate and individual tape-like terminal elements of different animals. Hairy attachment pads of insects, arachnids and reptiles were imaged using scanning electron microscopy (SEM) to analyze the contact geometry and the Kendall peeling model was employed to explain the reason for appearance of spatula-shaped terminal elements. The Kendall model has also been numerically studied by the Gao's group (Gao et al. 2005) and further extended in this important field of animal adhesion, by including the role of the pretension and for applications to hierarchical structures, in the papers by Chen et al. (2008, 2009).

In spite of this impressive, even if by force incomplete, fundamental literature, it is clear that multiple peeling clearly takes place in real, thus more complex, systems and requires the development of a new theory, of course with applications also in different fields, such as natural (e.g. spider silk) or artificial anchors. Such a theory is the aim of the present paper.

## 2 The theory of multiple peeling

Let us consider a three-dimensional complex system composed by $N$ adhesive tapes converging to a common point P, where an external force $\bar{F}$ is applied. Each tape has cross-section area $A_i$, Young modulus $Y_i$, length $l_i$ and orientation defined by the unitary vector $\bar{n}_i$, see Fig. 1.

The elastic displacement $\delta\bar{\eta}$ (assumed to be small, i.e. tape orientations do not change significantly) of the point P can be calculated with a classical approach as follows. The elongation of each tape is $\delta l_i = \delta\bar{\eta}\cdot\bar{n}_i$, thus the tape tension (if negative, the corresponding tape does not "work" and the external load is supported by the other tapes) is $\bar{T}_i = \delta l_i \bar{n}_i Y_i A_i/l_i = k_i \delta\bar{\eta}\cdot\bar{n}_i\bar{n}_i$, where $k_i = Y_i A_i/l_i$ is the tape stiffness. The equilibrium of the material point (hinge) P, where the load is applied, imposes $\sum_{i=1}^{N}\bar{T}_i = \bar{F}$ or equivalently $[K]\delta\bar{\eta} = \bar{F}$, where $[K]$ is the known (comparing the last two equations) stiffness matrix of the system. The elastic displacement $\delta\bar{\eta}$ is thus calculated as:

$$\delta\bar{\eta} = [K]^{-1}\,\bar{F} \tag{1a}$$

from which the tape elongations $\delta l_i$, tensions $T_i$ and strains $\varepsilon_i$ can be evaluated as:

$$\delta l_i = \delta\bar{\eta}\cdot\bar{n}_i,\ T_i = k_i\delta l_i,\ \ \varepsilon_i = \delta l_i/l_i,\quad i = 1,\ldots,N \tag{1b}$$

Imagine to impose a finite (the tape orientations change significantly) displacement $\Delta\bar{\eta}$ at the point P, to be accommodated by multiple *virtual* delaminations $\Delta l_i$ and elastic elongations of the tapes. A new global configuration, denoted by the symbol prime, takes place, see Fig. 2.

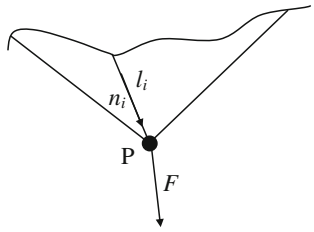


**Fig. 1** The multiple peeling system considered in this study

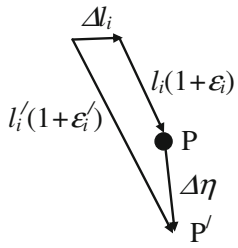


**Fig. 2** Finite delamination of the $i$th tape

From the scheme reported in Fig. 2 we deduce the validity of the following geometrical equations:

$$\bar{l}_i\,(1+\varepsilon_i)+\Delta\bar{l}_i+\Delta\bar{\eta}=\bar{l}_i'\left(1+\varepsilon_i'\right), \qquad (2)$$
$$\bar{l}_i=l_i\bar{n}_i,\ \bar{l}_i'=(l_i+\Delta l_i)\,\bar{n}_i',\quad i=1,\ldots,N$$

The strains $\varepsilon_i$ are known and their current values $\varepsilon_i'$ can be derived, according to Eq. (1), as a function of the unknown orientations $\bar{n}_i'$. Accordingly, coupling Eqs. (1b) and (2), we can write $4N$ scalar equations in $4N$ unknowns: the $N$ amplitudes of the virtual delaminations $\Delta l_i$ (their directions are known *a priori* from the configuration of the adhering tapes), the $N$ current strains $\varepsilon_i'$ and the $2N$ significant components of the new tape orientations $\bar{n}_i'(n_i'=1)$.

Inverting the previous problem, assuming as known three delamination amplitudes in Eq. (2), we could derive the other compatible delaminations as well the displacement $\Delta\bar{\eta}$ of the point P. This means that only three virtual delaminations can be considered as independent.

The virtual forces $F_i$ required for the delamination of the $i$th tape can be calculated by the Griffith's energy balance. Accordingly, the delamination takes place when:

$$-\partial\Pi/\partial l_i=2\gamma_i b_i,\ \Pi=E-W,\quad i=1,\ldots,N \qquad (3a)$$

where $\Pi$ is the total potential energy, $E$ is the elastic energy, $W$ is the external work, $\gamma_i$ is the surface energy of the $i$th tape/substrate interface and $b_i$ is its width.

The elastic energy variation can be calculated as:

$$\Delta E=\frac{1}{2}\sum_{i=1}^{N}A_iY_i\left(l_i'\varepsilon_i'^2-l_i\varepsilon_i^2\right) \qquad (3b)$$

The variation of the external work is:

$$\Delta W=\bar{F}\cdot\Delta\bar{\eta} \qquad (3c)$$

The real critical force is:

$$F_C=\min\{F_i\}=F_j \qquad (3d)$$

and corresponds to the delamination of the $j$th tape.

The algebraic system is nonlinear but can be linearized considering the differentials instead of the finite differences (e.g. $\Delta\bar{\eta}\rightarrow\mathrm{d}\bar{\eta}$). However note that the physical system remains intrinsically geometrically nonlinear due to the existence of the orientation variations. Moreover, the energy balance remains non linear in the force $F$.

## 3 The asymmetric V-shape-double peeling

The developed treatment is here applied to study a double peeling system, Fig. 3. From Eq. (1) we derive:

$$T_1=F\frac{\sin(\theta+\alpha_2)}{\sin(\alpha_1+\alpha_2)},\quad T_2=F\frac{\sin(\theta-\alpha_1)}{\sin(\alpha_1+\alpha_2)},$$
$$\varepsilon_i=T_i/(Y_iA_i) \qquad (4)$$

The previous equations are valid for $T_{1,2}>0$ thus for $\alpha_1<\theta<\pi-\alpha_2$. If a tension is negative only the other tape sustains the entire load and thus we have a classical single peeling (if both the tensions are negative the load cannot be in equilibrium).

From Eq. (2) we have:

$$\begin{cases} l_1\,(1+\varepsilon_1)\cos\alpha_1+\Delta l_1+\Delta u \\ \quad=(l_1+\Delta l_1)\left(1+\varepsilon_1'\right)\cos(\alpha_1+\Delta\alpha_1) \\ l_1\,(1+\varepsilon_1)\sin\alpha_1+\Delta v \\ \quad=(l_1+\Delta l_1)\left(1+\varepsilon_1'\right)\sin(\alpha_1+\Delta\alpha_1) \\ l_2\,(1+\varepsilon_2)\cos\alpha_2+\Delta l_2-\Delta u \\ \quad=(l_2+\Delta l_2)\left(1+\varepsilon_2'\right)\cos(\alpha_2+\Delta\alpha_2) \\ l_2\,(1+\varepsilon_2)\sin\alpha_2+\Delta v \\ \quad=(l_2+\Delta l_2)\left(1+\varepsilon_2'\right)\sin(\alpha_2+\Delta\alpha_2) \\ \varepsilon_1'=\dfrac{F}{Y_1A_1}\dfrac{\sin(\theta+\alpha_2+\Delta\alpha_2)}{\sin(\alpha_1+\alpha_2+\Delta\alpha_2+\Delta\alpha_1)} \\ \varepsilon_2'=\dfrac{F}{Y_2A_2}\dfrac{\sin(\theta-\alpha_1-\Delta\alpha_1)}{\sin(\alpha_1+\alpha_2+\Delta\alpha_2+\Delta\alpha_1)} \end{cases} \qquad (5)$$

where $\Delta u$ and $\Delta v$ are the horizontal and vertical components of the displacement $\Delta\bar{\eta}$. Note that the classical single peeling only requires one equation, since no angle and strain variations occur during delamination.

Considering $\Delta\varepsilon_i=\varepsilon_i'-\varepsilon_i$ and solving the previous system in the limit of small variations (i.e. substituting the finite differences with the differentials), yields:

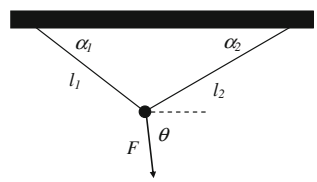


**Fig. 3** The double peeling system

$$[A] = \begin{bmatrix} 1 & 0 & l_1(1+\varepsilon_1)\sin\alpha_1 & 0 & -l_1\cos\alpha_1 & 0 \\ 0 & 1 & -l_1(1+\varepsilon_1)\cos\alpha_1 & 0 & -l_1\sin\alpha_1 & 0 \\ -1 & 0 & 0 & l_2(1+\varepsilon_2)\sin\alpha_2 & 0 & -l_2\cos\alpha_2 \\ 0 & 1 & 0 & -l_2(1+\varepsilon_2)\cos\alpha_2 & 0 & -l_2\sin\alpha_2 \\ 0 & 0 & \sin(\theta+\alpha_2)\cos(\alpha_1+\alpha_2) & \sin(\theta-\alpha_1) & \sin^2(\alpha_1+\alpha_2)\,Y_1A_1/F & 0 \\ 0 & 0 & \sin(\theta+\alpha_2) & \sin(\theta-\alpha_1)\cos(\alpha_1+\alpha_2) & 0 & \sin^2(\alpha_1+\alpha_2)\,Y_2A_2/F \end{bmatrix} \tag{6a}$$

$$[b_1] = \begin{bmatrix} (1+\varepsilon_1)\cos\alpha_1 - 1 \\ (1+\varepsilon_1)\sin\alpha_1 \\ 0 \\ 0 \\ 0 \\ 0 \end{bmatrix}, \quad [b_2] = \begin{bmatrix} 0 \\ 0 \\ (1+\varepsilon_2)\cos\alpha_2 - 1 \\ (1+\varepsilon_2)\sin\alpha_2 \\ 0 \\ 0 \end{bmatrix}, \quad [\mathrm{d}x] = \begin{bmatrix} \mathrm{d}u \\ \mathrm{d}v \\ \mathrm{d}\alpha_1 \\ \mathrm{d}\alpha_2 \\ \mathrm{d}\varepsilon_1 \\ \mathrm{d}\varepsilon_2 \end{bmatrix} \tag{6b}$$

$$[\mathrm{d}x] = [A]^{-1}\left([b_1]\,\mathrm{d}l_1 + [b_2]\,\mathrm{d}l_2\right) \tag{6c}$$

Equation (3b) in the limit of small variations, gives:

$$\mathrm{d}E = Y_1A_1l_1\varepsilon_1\mathrm{d}\varepsilon_1 + Y_2A_2l_2\varepsilon_2\mathrm{d}\varepsilon_2 + \frac{1}{2}Y_1A_1\varepsilon_1^2\mathrm{d}l_1 + \frac{1}{2}Y_2A_2\varepsilon_2^2\mathrm{d}l_2 \tag{7}$$

as well as Eq. (3c) poses:

$$\mathrm{d}W = F\cos\theta\,\mathrm{d}u + F\sin\theta\,\mathrm{d}v \tag{8}$$

According to Eq. (3a) and (3d) the delamination force can thus be obtained.

## 4 The symmetric cone-shape-multiple peeling, including large deformations and pre-stretching

To further simplify the equations, let us considering the symmetric case ($\alpha_1 = \alpha_2 = \alpha, l_1 = l_2 = l, \theta = \pi/2$, and consequently $u = 0$ and $\varepsilon_1 = \varepsilon_2 = \varepsilon$); we accordingly find the following solutions:

$$\begin{aligned}\mathrm{d}\varepsilon &= \frac{1-(1+\varepsilon)\cos\alpha}{\frac{1+\varepsilon}{\varepsilon}\frac{\sin^2\alpha}{\cos\alpha}+\cos\alpha}\frac{\mathrm{d}l}{l} \\ &= \left[\frac{(1-\cos\alpha)\cos\alpha}{\sin^2\alpha}\varepsilon + \left(\frac{\cos^2\alpha}{\sin^4\alpha} - \frac{\cos^2\alpha}{\sin^2\alpha} - \frac{\cos\alpha}{\sin^4\alpha}\right)\varepsilon^2 + O\left(\varepsilon^3\right)\right]\frac{\mathrm{d}l}{l}\end{aligned} \tag{9a}$$

$$\begin{aligned}\mathrm{d}\alpha &= \frac{[(1+\varepsilon)\cos\alpha - 1]\,\mathrm{d}l + l\cos\alpha\mathrm{d}\varepsilon}{l(1+\varepsilon)\sin\alpha} \\ &= \left\{\frac{[(1+\varepsilon+l\mathrm{d}\varepsilon/\mathrm{d}l)\cos\alpha - 1]\left(1-\varepsilon+\varepsilon^2\right)}{\sin\alpha} + O\left(\varepsilon^3\right)\right\}\frac{\mathrm{d}l}{l}\end{aligned} \tag{9b}$$

$$\mathrm{d}v = l(1+\varepsilon)\cos\alpha\mathrm{d}\alpha + l\sin\alpha\mathrm{d}\varepsilon + (1+\varepsilon)\sin\alpha\mathrm{d}l \tag{9c}$$

Neglecting the terms $O\left(\varepsilon^3\right)$, the energy balance is self-consistently written considering terms up to the third power of $\varepsilon$, as required for treating large deformations. We have verified that the energy balance remains valid also for the symmetric cone-shape multiple peeling of $N$ adhesive tapes, that generalizes the symmetric double peeling ($N = 2$). We can further generalize the result considering the presence of a pre-stretching $\varepsilon_0$ of the tapes, following Chen et al. (2009); we finally find:

$$\beta(\alpha,\varepsilon_0)\,\varepsilon^3 + \varepsilon^2 + 2(1-\cos\alpha-\varepsilon_0)\,\varepsilon - 4\lambda + \varepsilon_0^2 = 0, \quad \text{where } \lambda = \frac{\gamma}{tY} \tag{10a}$$

where $\beta(\alpha,\varepsilon_0)$ is a known function and $t = A/b$ is the tape thickness. Equation (10a) can be solved in closed form. In particular, for not too large deformations the critical values of the strain $\varepsilon_C$ for peeling are obtained as:

$$\varepsilon_C = \varepsilon_{C-}, \varepsilon_{C+} = -1 + \cos\alpha + \varepsilon_0 \mp \sqrt{(1-\cos\alpha-\varepsilon_0)^2 + 4\lambda - \varepsilon_0^2}. \tag{10b}$$

Equation (10b) indicates that stable adhesion is possible only for $\max(\varepsilon_{C-}, 0) < \varepsilon < \varepsilon_{C+}$. In the case of small pre-stretching $\varepsilon_{C-} < 0$, and stable adhesion requires $0 < \varepsilon < \varepsilon_{C+}$; whereas for large pre-stretching $\varepsilon_{C-} > 0$, and stable adhesion implies $\varepsilon_{C-} < \varepsilon < \varepsilon_{C+}$. In this case, the detachment occurs not only for large stretching, when $\varepsilon \geq \varepsilon_{C+}$, but also for small stretching, when $\varepsilon \leq \varepsilon_{C-}$. This implies that, in the case

of very large pre-stretching, a finite applied stretching is actually necessary to stabilize adhesion, otherwise the pre-stretching will be alone sufficient to detach the film. For a detailed analysis on the influence of the pre-tension see the paper by Chen et al. (2009).

We note that the previous equation (where we have neglected the terms $O(\varepsilon^2)$ for direct comparison with the Kendall's approach) is surprising: it is identical to that of the single peeling problem. *Accordingly, the analysis suggests to treat the multiple peeling as independent single peeling processes, considering each tape loaded by its tension* (*remark 1*). This approximation corresponds to assuming the validity of the free body diagram. This is not trivial, since peeling involves energy balance (particularly, surface energy dissipation) and not just force equilibrium. This "free body diagram approximation" drastically reduces the complexity in treating the multiple peeling, e.g. allowing us to easily study non symmetric configurations of the tapes and of the load.

Thus, the force predicted for multiple peeling, different with respect to that of single peeling ($F_C = YA\varepsilon_C$), is:

$$F_C = NYA \sin\alpha\varepsilon_C \tag{11}$$

Note that for soft tapes and vanishing pre-stretching:

$$F_C \approx 2bN \sin\alpha\sqrt{\gamma t Y} \tag{12a}$$

whereas for rigid tapes and vanishing pre-stretching:

$$F_C \approx \frac{2bN\gamma \sin\alpha}{1-\cos\alpha} \tag{12b}$$

The behaviour described by Eq. (11) is depicted in Fig. 4. *An angle for maximal adhesion* $\alpha_{\max}$ *clearly emerges, as a function of the parameter* $\lambda$ (*remark 2*). Figure 4 shows that the optimal angle disappears (tends to zero) for rigid tapes (Eq. 12b) but it is expected to be observable and tending to 90 degrees for soft tapes (Eq. 12a). This is exactly what we have preliminary (work in progress) observed in vitro (experiments on soft adhesive tapes, from Pugno and Gorb 2009) and in silico (atomistic simulations of graphene anchorages, from Pugno et al. 2011).

## 5 Gecko adhesion and spider silk anchors

The angle for maximal adhesion could thus be used in Nature by animals to maximize adhesion at all the different hierarchical levels, in controlateral legs, digits and even setae (Fig. 5). In formulae this optimization could be written as:

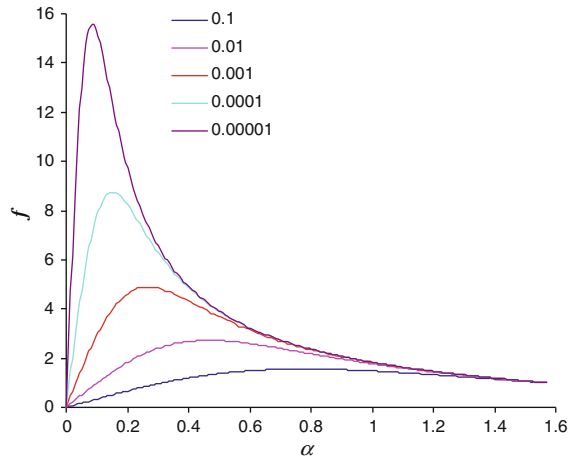


**Fig. 4** Dimensionless force $f = F_C(\alpha)/F_C(\alpha = \pi/2)$ versus angle $\alpha$ by varying the dimensionless adhesion strength $\lambda$ and for vanishing pre-stretching; $F_C\ (\alpha = \pi/2) = NYA(-1 + \sqrt{1+4\lambda})$

$$Opt : \alpha_{opt}^{(i)} = \alpha_{\max}^{(i)}. \tag{13}$$

Equation (13) should be valid at each hierarchical level $i$.

But how these optimal angles can be reached? A "smart mechanism" is suggested by Eq. (11) and Fig. 4, which show that it is sufficient to increase the load in order to increase or decrease the angle and automatically reach its optimal value and thus the maximal adhesion.

This optimal angle could also be used by Nature to optimize the strength of natural anchors. For example we noted a V-shape hierarchical geometry in the spider anchors, from the macro- to the micro-scale (Fig. 6). The Scanning Electron Microscope (SEM) Images in Fig. 6b shows a microscale V-shaped anchor lying in the plane of the contact surface, thus different than the V-shaped configuration that we have treated in Sect. 4 and observable in Fig. 6a. However, note that the observed SEM architecture can be treated by the general theory, Sect. 2, even in a simple way by invoking the "free body diagram approximation". Moreover, we cannot exclude that the anchor originally was out of the plane, but made to collapse to the contact surface during manipulation.

Of course, in order to preserve life, animals are not interested in having the adhesion strength comparable to the intrinsic fracture strength $\sigma_f$ of their constituents.

**Fig. 5** The angle for maximal adhesion could be used by geckos to maximize adhesion at all the different hierarchical levels, in controlateral legs, digits and even setae

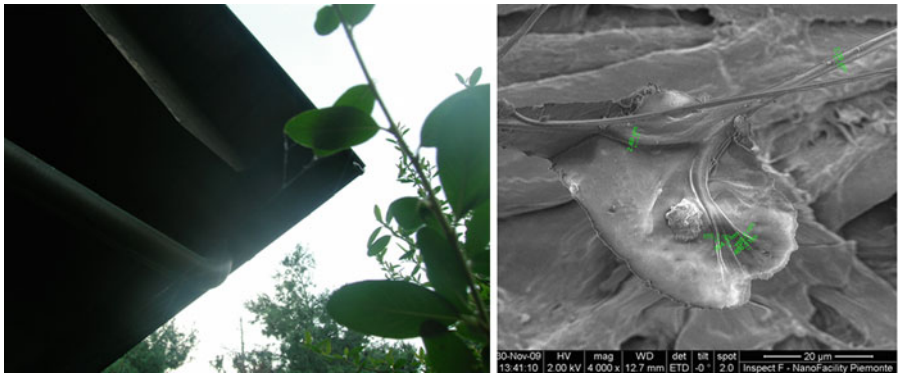

**Fig. 6** Spider anchors are often V-shaped and hierarchical in nature. Two-level hierarchical V-shape can be recognized at the macroscopic size-scale (*left*) whereas even more hierarchical levels emerge at the microscale (*right*)

On the other hand, this condition could be ideal for optimizing natural anchors, e.g. those of spiders. *Thus, for "uniform strength" optimized anchors, we require the simultaneous failure of all the "tapes" and of the detachment itself* (*remark 3*); in formulae:

$$Opt : \sigma^{(i)}\,(F = F_C) = \sigma_f^{(i)} \tag{14}$$

where the superscript $i$ denotes different tapes, even at different hierarchical levels. Equation (14) leads to different optimized geometries, even very complex (that will be discussed in a subsequent paper). Here let us discuss in the following only the simplest case, resulting in the definition of an optimal number of adhesive contacts.

Defining the nominal peeling strength as $\sigma_C = F_C/(NA)$ we expect $\sigma_C \propto t^{-1/2}$ for soft tapes (see Eq. 12a) whereas $\sigma_C \propto t^{-1}$ for rigid tapes (Eq. 12b). Accordingly, splitting a tape with thickness $t$ into $n$ thinner subtapes, i.e. $t \to t/n$, increases the total peeling strength (or force) by a factor of $\sqrt{n}$ or $n$ respectively (or, in general, in between). Similarly, splitting the cross-sectional area of the tape into $n$ subareas, i.e. $t \to t/\sqrt{n}$, would lead to increment of $\sqrt{n}$ or $\sqrt{\sqrt{n}}$, respectively.

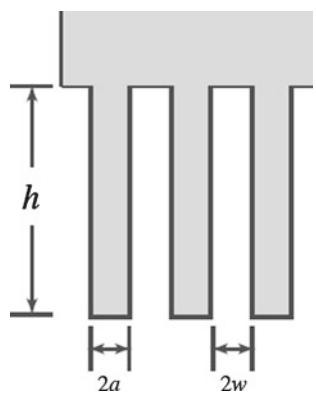


**Fig. 7** A micro-structured tape

Of course, splitting only the width tape ($t = \text{const}$) does not affect the strength. Thus, in general:

$$\sigma_C(n) \approx \sigma_C(n=1) \times n^{\lambda}, \quad 0 \le \lambda \le 1 \tag{15a}$$

with:

$$\begin{cases} \lambda = 1, & \textit{rigid } \& \; t \to t/n \\ \lambda = 1/2, & \textit{rigid } \& \; t \to t/\sqrt{n} \quad \textit{or} \quad \textit{soft } \& t \to t/n \\ \lambda = 1/4, & \textit{soft } \& \; t \to t/\sqrt{n} \\ \lambda = 0, & \textit{rigid or soft } \& \; t = \textit{const} \end{cases} \tag{15b}$$

The scaling of $\lambda = 1/2$ was firstly found in the contact of a cylindrical geometry (Arzt et al. 2003) and invoked to explain the huge number of terminal units observed in adhesive based animals. Similarly, the same scaling exponent has been demonstrated for the area-splitting of a rigid tape (second case in Eq. 15b), to treat more realistically the two dimensional geometry of the spatulae observed in the pads of the adhesive based animals (Varenberg et al. 2010). Thus increasing the contacts number increases the adhesive strength (smaller is stronger), but with a different power of the scaling law, as dictated by the considered material stiffness and splitting geometry. Note that, since we are considering the same area, Eq. (15a) could also be rewritten in terms of force, i.e. $F_C(n) \approx F_C(n=1) \times n^{\lambda}$.

Denoting with $\sigma_F = F_f/(NA)$ the applied nominal stress corresponding to the intrinsic fracture, Eq. (14) could be rewritten in terms of nominal stresses as $\sigma_F = \sigma_C(n)$, from which an optimal contacts number emerges:

$$n_{opt} \approx \sqrt[\lambda]{\frac{\sigma_F}{\sigma_C(n=1).}} \tag{16}$$

Equation (16) could have a role for understanding the optimal splitting in spider silk anchors (work in progress) or even in the design of super-strong materials (Pugno 2010).

## 6 Peeling process zone length, flaw-tolerant peeling and pre-stretching to control adhesion of a micro-structured tape

In order to evaluate the length of the peeling process zone, we simply calculate here the contact stress distribution according to the classical elastic solution for a rectangular beam cross-section. We obtain:

$$\tau(y) \approx \frac{6T\cos\alpha}{S}\left(\frac{1}{4} - \left(\frac{y}{l}\right)^2\right) \tag{17a}$$

$$\sigma(y) = \frac{T\sin\alpha}{S} + \frac{6T\sin\alpha}{S}\frac{y}{l} \tag{17b}$$

where $y = 0$ is placed at the middle line of the contact, $T$ is the tape tension and $S$ is the contact surface area.

The equivalent stress, assuming the Tresca criterion is $\sigma_{eq}(y) \approx \sqrt{\sigma^2(y) + 4\tau^2(y)}$ (according to the von Mises criterion the factor 4 must be replaced by 3) and the maximal (local or absolute) value $\sigma_{eq}^{(\max)}$ can be easily numerically calculated. We find the following approximated solution (asymptotic matching, exact for $\theta = 0, \pi/2, \pi$):

$$\sigma_{eq}^{(\max)} \approx \sqrt{\sigma^{(\max)} + 4\tau^{(\max)}} = \sqrt{9 + 5\sin^2\alpha}\frac{T}{S} \tag{18}$$

Accordingly, the process zone length $l_c = S/b$ can be calculated inserting in Eq. (18) $\sigma_{eq}^{(\max)} = \sigma_a$, that is the adhesive strength, and $T = T_c = Ebt\varepsilon_c$, that is the critical tape tension for peeling; we find:

$$l_c(\alpha) \approx \sqrt{9 + 5\sin^2\alpha}\frac{E\varepsilon_c(\alpha)}{\sigma_a}t \tag{19}$$

Consequently, the longer the process zone the larger the peeling force and for $l > l_c^{(\max)}$ the peeling force becomes maximal and peeling becomes flaw-tolerant (note that Eq. (19) defines a critical slenderness, thus a minimal contact length or, equivalently, a maximal tape thickness). Thus, in order to increase adhesion and to reduce the occupied surface (i.e. to increase the number of contacts and thus again adhesion) we expect $l^{(opt)} \approx l_c^{(\max)}$. Inserting plausible values of a gecko spatula in Eq. (19) ($E \approx 1$ GPa for gecko keratin, $\sigma_a \approx 1$ MPa for van der Waals adhesion, $\varepsilon_a^{(\max)} \approx 0.1$ for the peeling strain and $t \approx 10$ nm for the spatula thickness) results in $l_c^{(\max)} \approx 387$ nm, close to the real length of a gecko spatula [see Fig. 2 in Pantano et al. (2011), this Special Section]. This suggests that the peeling of insects, lizards and spiders is flaw-tolerant. Also, note that solving $\tau_{\max}(\alpha) = \sigma_{\max}(\alpha)$ leads to $\alpha = \alpha_c \approx 21°$; thus for $\alpha < \alpha_c$ one would expect a sliding more than a real peeling, as experimentally observed in geckos (Gao et al. 2005).

Finally, let us consider a micro-structured tape, with vertically aligned tiny cylindrical fibres of height $h$ and spaced by $2w$, Fig. 7 (with self-adhesive, e.g. van der Waals, energy $\gamma_f$, Young's modulus $Y_f$ and Poisson's ratio $\nu_f$); the pre-stretching can tune the effective distance between the hairs and can thus smartly control theirs anti-bunching/bunching transition and consequently the adhesive/anti-adhesive property of the bio-inspired tape; following Glassmaker et al. (2004), we find the following switching strain:

$$\varepsilon_c^{(switching)} = \frac{h^2}{w}\beta\left(\frac{\gamma_f}{12Y_f a^3}\right)^{1/2} - 1 \tag{20}$$

where:

$\beta = 1$ for rectangular cross-section, with non contacting sides of length $2a$, Fig. 7

or:

$\beta = \left(\frac{2^{11}\gamma_f(1-\nu_f^2)}{\pi^4 Y_f a}\right)^{1/6}$ for circular cross-section, of diameter $2a$.

Nature could perhaps be aware of this concept and in any case nanotechnology can be inspired by it.

## 7 Conclusion

In this paper we have solved the multiple peeling problem (including large deformations and pre-stretching). We have surprisingly observed: (1) a governing equation for the strain identical to that of the single peeling, (2) an optimal peeling angle, at which adhesion is maximal, that can be reached in a smart way simply by increasing the tensile force; finally, a hierarchical optimization and uniform strength anchor design have been introduced (3). Such results could be of great importance for better understanding biological adhesive systems or anchorages, as well as for the design of bio-inspired super-adhesive smart materials or super-strong anchors. Also, the length of the peeling process zone is calculated, suggesting an optimal value for maximal and flaw-tolerant adhesion; finally, a new pre-stretching mechanism is discussed to smartly control the adhesion of bio-inspired hairy tapes.

**Acknowledgments** NMP is supported by the Regione Piemonte, Italy (METREGEN, 2009–2012: " Metrology on a cellular and macromolecular scale for regenerative medicine "). NMP thanks H. Gao for discussion, specifically on Sect. 6.

## References

Arzt E, Gorb S, Spolenak R (2003) From micro to nano contacts in biological attachment devices. Proc Natl Acad Sci USA 100:10603–10606

Autumn K, Peattie AM (2002) Mechanisms of adhesion in geckos. Integr Comp Biol 42:1081–1090

Autumn K, Sitti M, Liang YA, Peattie AM, Hansen WR, Sponberg S, Kenny TW, Fearing R, Israelachvili JN, Full RJ (2002) Evidence for van der Waals adhesion in gecko setae. Proc Natl Acad Sci USA 99:12252–12256

Bhushan B, Sayer A (2007) Gecko feet: natural attachment systems for smart adhesion Applied Scanning Probe Methods vol VII, Biomimetics and Industrial Applications. Springer, Berlin 41–76

Chen B, Wu P, Gao H (2008) Hierachical modeling of attachment and detachment mechanisms of gecko toe adhesion. Proc R Soc A 464:1639–1652

Chen B, Wu P, Gao H (2009) Pre-tension generates strongly reversible adhesion of a spatula pad on substrate. J R Soc Interface 6:529–537

Chen S, Gao H (2007) Bio-inspired mechanics of reversible adhesion: orientation-dependent adhesion strength for non-slipping adhesive contact with transversely isotropic elastic materials. J Mech Phys Solids 55:1001–1015

Eisner T, Aneshansley DJ (2000) Defense by foot adhesion in a beetle (Hemisphaerota cyanea). Proc Natl Acad Sci USA 97:6568–6573

Federle W, Rohrseitz K, Holldobler B (2000) Attachment forces of ants measured with a centrifuge: better 'waxrunners' have a poorer attachment to a smooth surface. J Exp Biol 203:505–512

Gao H, Wang X, Yao H, Gorb S, Arzt E (2005) Mechanics of hierarchical adhesion structures of geckos. Mech Mater 37:275–285

Geim AK, Dubonos SV, Grigorieva IV, Novoselov KS, Zhukov AA, Shapoval SY (2003) Microfabricated adhesive mimicking gecko foot-hair. Nat Mater 2:461–463

Glassmaker NJ, Jagota A, Hui CY, Kim J (2004) Design of biomimetic fibrillar interface: 1. Making contact. J R Soc Lond Interface 1:23–33

Gorb SN (2001) Attachment devices of insect cuticle. Kluwer, Dordrecht

Huber G, Gorb SN, Spolenak R, Arzt E (2005) Resolving the nanoscale adhesion of individual gecko spatulae by atomic force microscopy. Biol Lett 1:2–4

Huber G, Mantz H, Spolenak R, Mecke K, Jacobs K, Gorb SN, Arzt E (2005) Evidence for capillarity contributions to gecko adhesion from single spatula and nanomechanical measurements. Proc Natl Acad Sci USA 102:16293–16296

Israelachvili JN (1991) Intermulecular and surface forces with application to colloidal and biological systems (Colloid Science S; NewYork: Academic press)

Johnson KL, Kendall K, Roberts AD (1971) Surface energy and the contact of elastic solids. Proc R Soc A 324:301–313

Kendall K (1975) Thin-film peeling-elastic term. J Phys D Appl Phys 8:1449–1452

Kesel AB, Martin A, Seidl T (2004) Getting a grip on spider attachment: an AFM approach to microstructure adhesion in arthropods. Smart Mater Struct 13:512–518

Pantano A, Pugno NM, Gorb S (2011) Numerical simulations demonstrate that the double tapering of the spatualae of lizards and insects maximize both detachment resistance and stability. Int J Fract. doi:10.1007/s10704-011-9596-8

Pugno N (2007a) Velcro® nonlinear mechanics. Appl Phys Lett 90:121918

Pugno N (2007b) Towards a Spiderman suit: large invisible cables and self-cleaning releasable super-adhesive materials. J Phys Cond Mat 19:395001 (17 pp)

Pugno N (2008) Spiderman gloves. Nano Today 3:35–41

Pugno N (2010) The design of self-collapsed super-strong nanotube bundles. J Mech Phys Solids 58:1397–1410

Pugno N, Gorb S (2009) Functional mechanism of biological adhesive systems described by multiple peeling approach. In: Proceedings of the 12th international conference on fracture, July 12–17, Ottawa, Canada, USA

Pugno N, Lepore E (2008a) Observation of optimal gecko's adhesion on nanorough surfaces. Biosystems 94:218–222

Pugno N, Lepore E (2008b) Living tokay geckos display adhesion times following the Weibull statistics. J Adhesion 84:949–962

Pugno N, Vanzo J, Buehler M (2011) Self-strengthening of graphene anchorages, GRAPHITA Proceedings, 15–18 May 2011, Gran Sasso National Laboratories (Assergi-L'Aquila), Italy

Varenberg M, Pugno N, Gorb S (2010) Spatulae structures in biological fibrillar adhesion. Soft Matter 6:3269–3272

Yao H, Gao H (2006) Mechanics of robust and releasable adhesion in biology: bottom-up designed hierarchical structures of gecko. J Mech Phys Solids 54:1120–1146